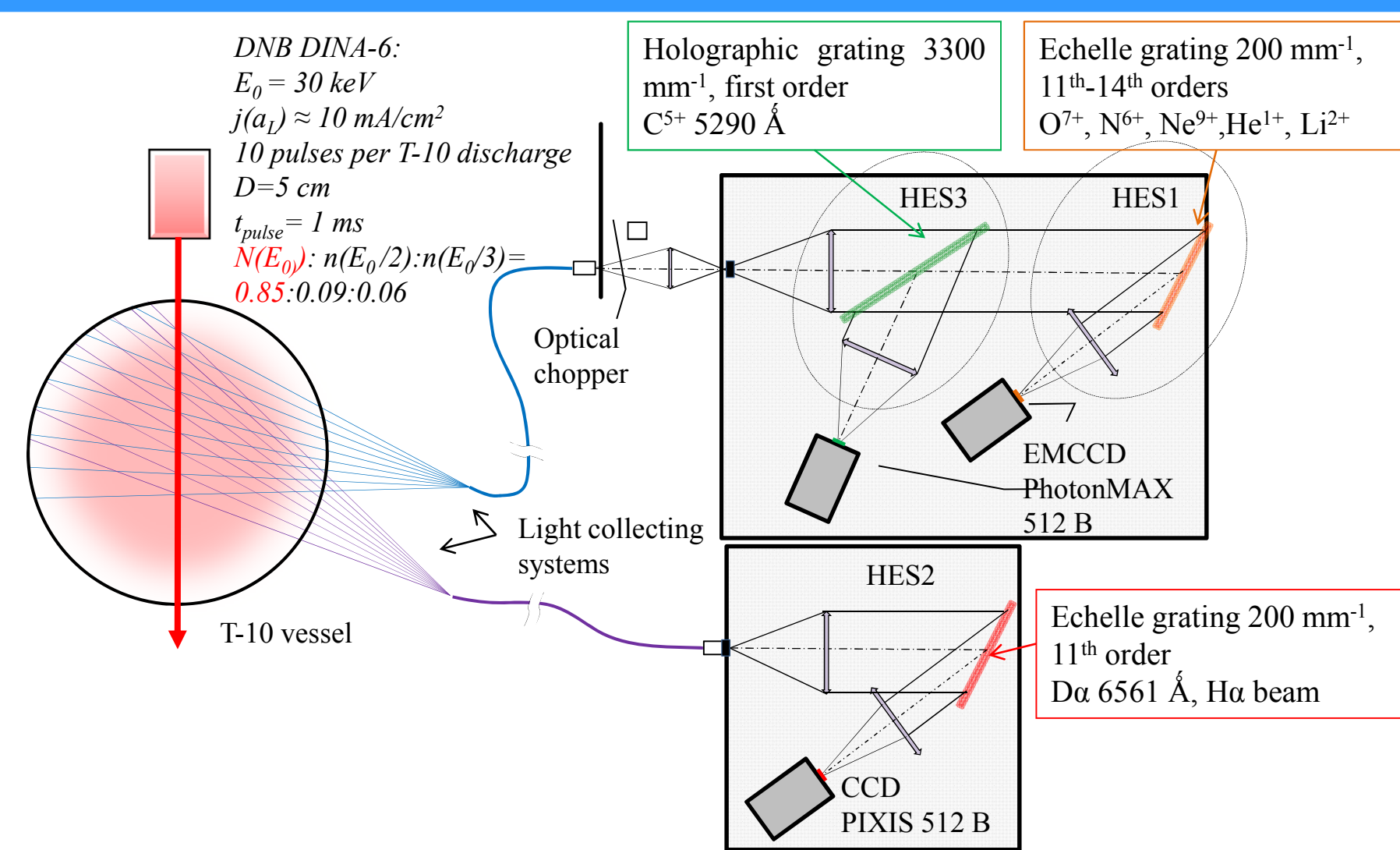


INTRODUCTION

Experimental study of the impurity removal from the central plasma region after ECR heating switching on is carried out. The neoclassical impurity accumulation is observed at high Z_{eff} conditions of T-10 plasma in discharges with the high electron density and the low plasma current. Transport calculations with the neoclassical and anomalous diffusion coefficients for fully ionized impurity, are provided to describe the impurities density profiles measured by CXRS diagnostics in various regimes. The central ECR heating leads to the efficient flattening of the impurities density profiles when the neoclassical transport is dominant at the Ohmic phase. Thus, the experiment demonstrates the direct link between the impurity removal effectiveness using ECR heating and the value of the impurity density gradient in the OH plasma. Measured impurity dynamics during the ECRH switch on transient phase allows to make transport calculations and to estimate anomalous transport coefficients in the ECRH regime. The anomalous diffusion coefficient for the fully ionized impurity increases after switching on 1 MW ECRH that is shown by the transport modeling of the impurity removal dynamics. According to the CXRS measurements, during first several tens of milliseconds after ECRH switching on fully ionized impurity removal occurs only in the central region of plasma (probably inside the r_s region). It is noticed that the amount of carbon and oxygen particles removed from the central region corresponds to the amount of electrons removed by the density pump-out effect implying the quasineutrality condition. The fact that plasma deuterons weakly participate in the particle removal process is possibly due to the flat deuteron density profile in the central region and thus deuterons have low sensitivity to the anomalous diffusion increase. Analysis of possibility of the impurity removal dynamics application to the study of density pump-out effect is carried out.

CXRS diagnostics



- 2 CXRS spectra of impurities and H α beam line simultaneously
- 9 spatial points with 2-4 cm spatial resolution
- 1 ms temporal resolution
- Measurements of bremsstrahlung chord profile

Impurity density profiles in Ohmic discharges with high plasma current

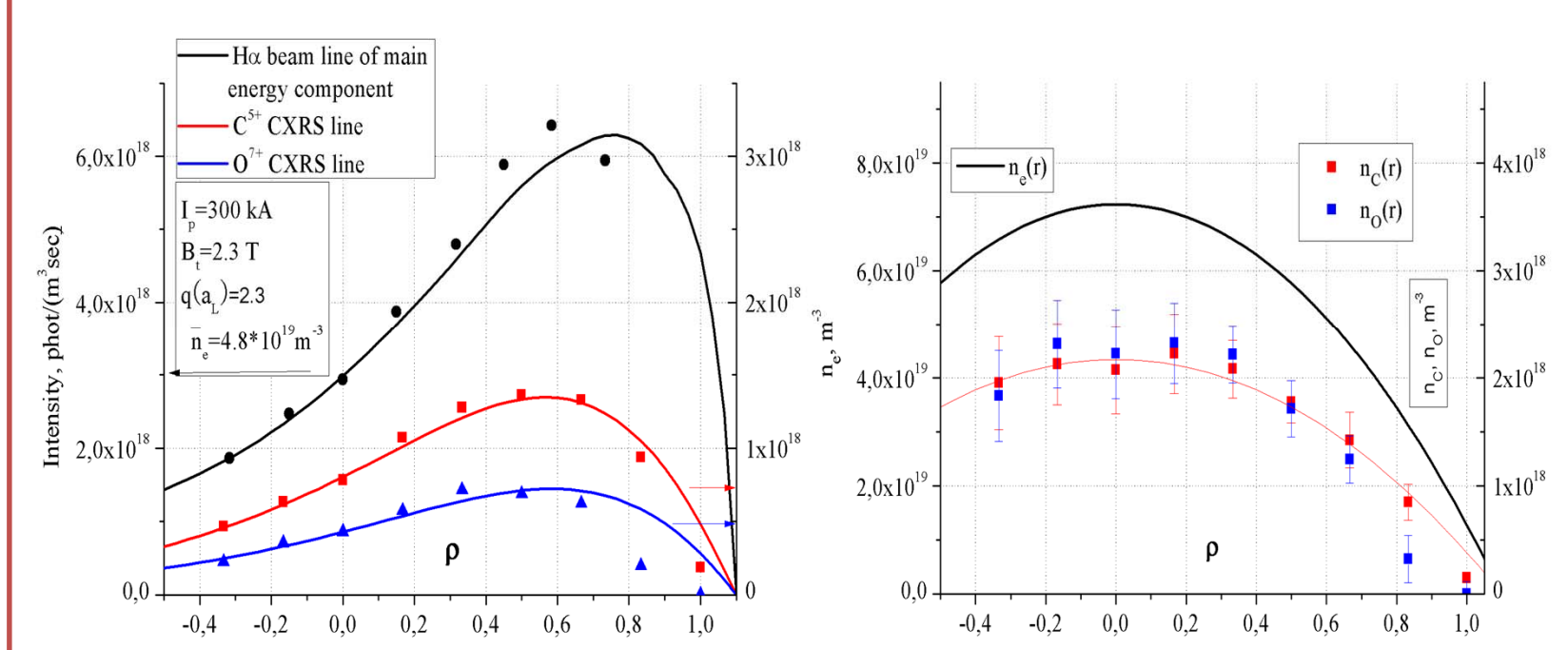


FIG. 1. A – distribution of CXRS signals along beam path in OH discharge with $I_p=300$ kA. Points – experiment, lines – model of beam propagation and line emissivity, based on ADAS data. B – measured radial profiles of carbon and oxygen nuclei concentrations. The calculated fractions of carbon and oxygen nuclei are: $\delta C=3\%$ and $\delta O=3\%$. Estimated values of $Z_{\text{eff}} \approx 3.5 = \text{const}(r)$ are in good agreement with bremsstrahlung measurements. Discrepancies are observed only at the plasma periphery where carbon and oxygen nuclei can be charge-exchanged on the deuterium atoms. It is important to note that impurity density profiles are similar with $n_e(r)$, indicating the domination of the anomalous transport.

Impurities density profiles peaking in OH plasma

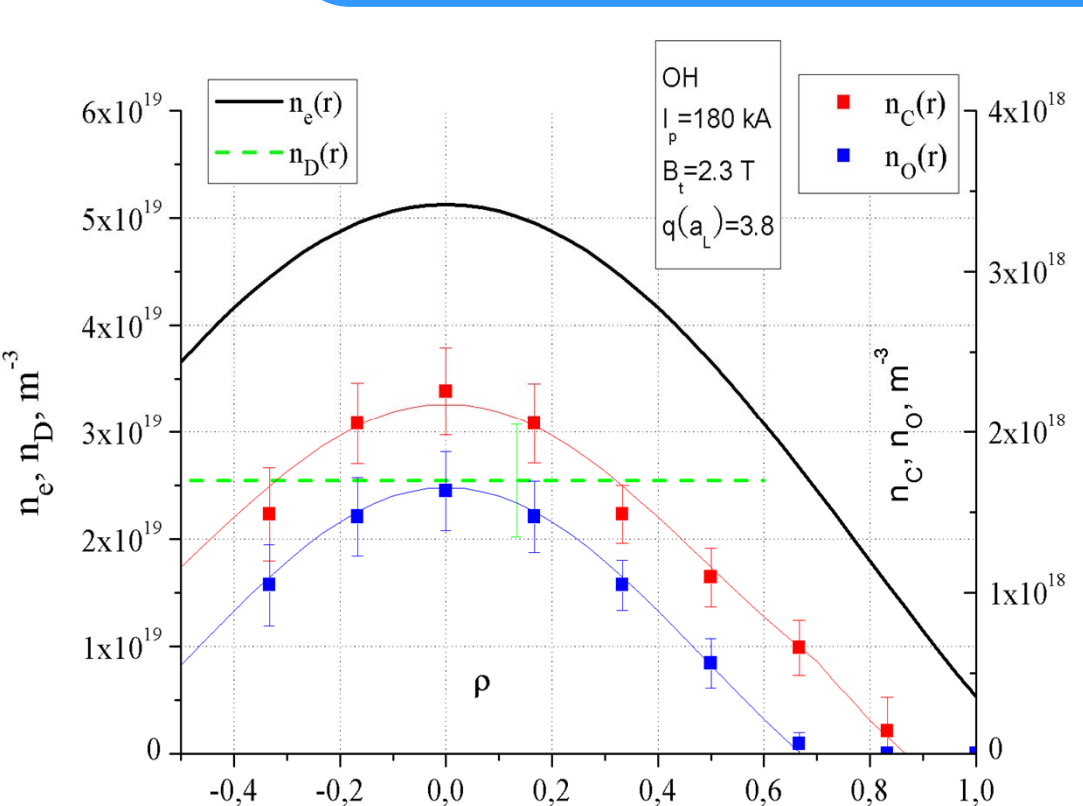


FIG. 2. Measured radial profiles of carbon and oxygen nuclei concentrations in OH discharge with $I_p=180$ kA. Estimated deuterons concentration is shown by green line.

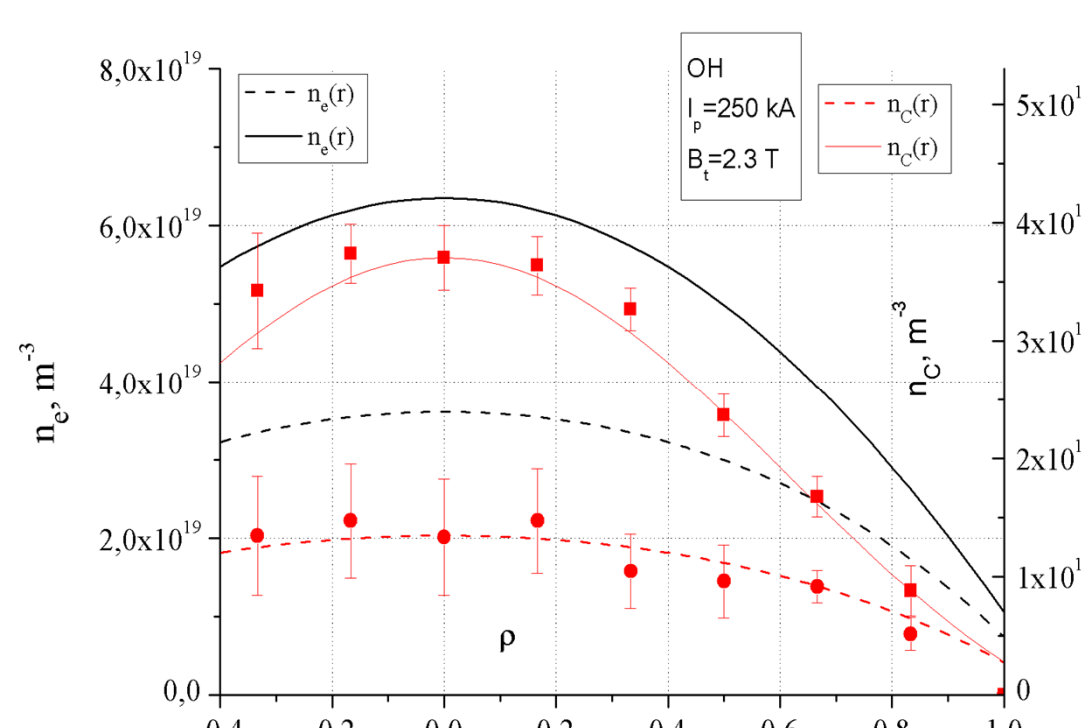


FIG. 3. Measured radial profiles of carbon nuclei concentrations in OH discharges with $I_p=250$ kA at two different electron densities.

FIG. 4. A – Temporal evolution of radial profiles of electron density in OH discharge with $I_p=180$ kA. B – Temporal evolution of radial profiles of carbon nuclei profiles.

FIG. 5. Temporal evolution of chord profiles plasma radiation, measured by different diagnostics OH discharge with $I_p=180$ kA. A – bremsstrahlung, B – SXR, C – AXUV

Modeling in transport code

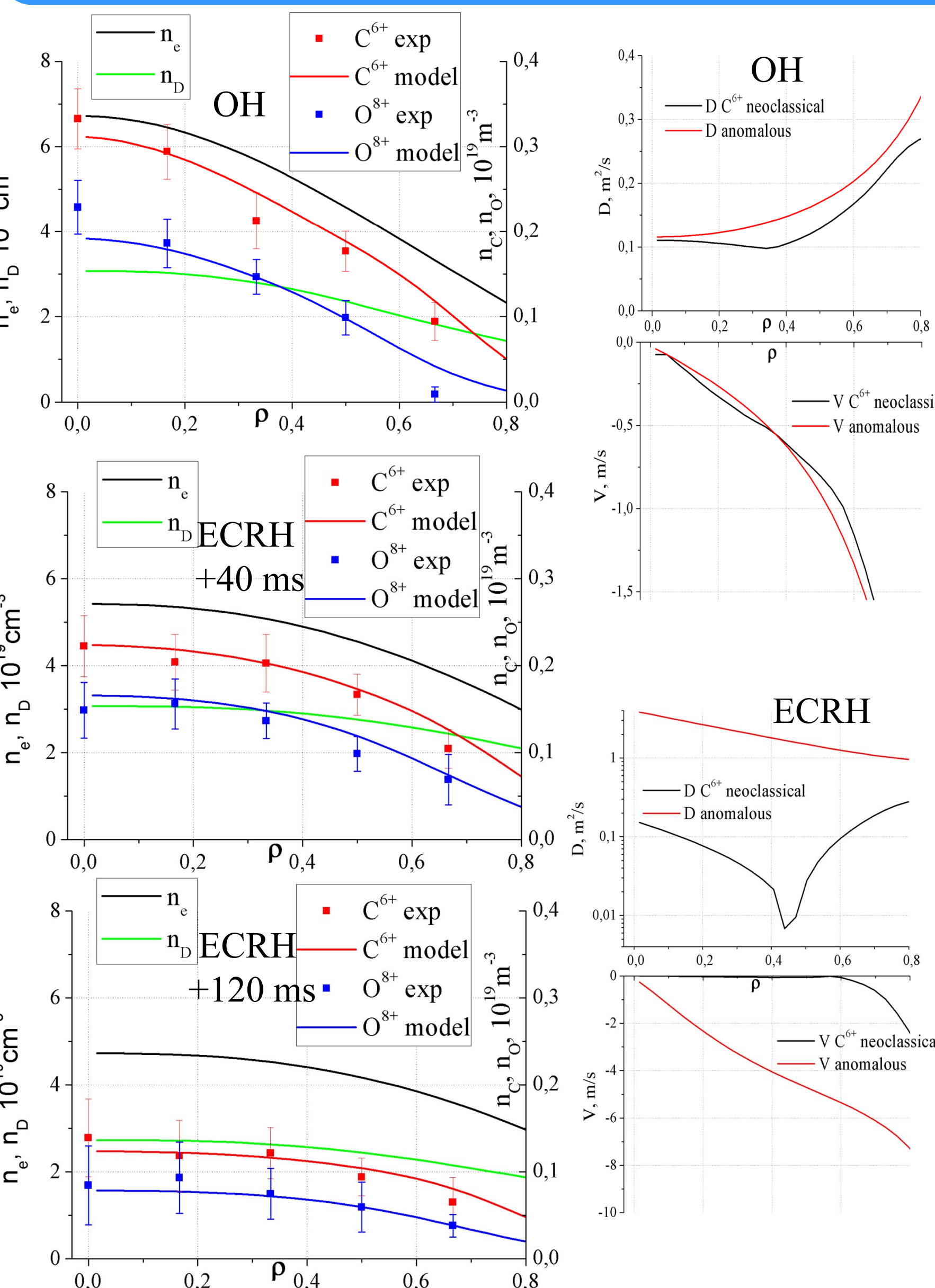


FIG. 12. Modeling of carbon and oxygen concentrations in discharge with $I_p=180$ kA in OH plasma and in ECRH regime with $P_{\text{ECRH}}=1$ MW

Transport codes are used for evaluation of transport coefficients, describing time dynamics of radial profiles of impurities in transition from steady state in OH plasma to steady state in ECRH plasma and both steady states, including neoclassical and anomalous transport. Transport code allows simulating behavior of two impurities simultaneously, for example – carbon and oxygen, including impurity-impurity collisions, that is important for high values of Z_{eff} . In earlier experiments it has been shown in that next expressions can be used for anomalous impurity transport in OH plasma of T-10:

$$D_{\text{an}}^{\text{exp}}(r) = \frac{2}{n_e(r) \cdot Z_{\text{eff}}} n_i^2 / s, \quad V_{\text{an}}^{\text{exp}}(r) = D_{\text{an}}^{\text{exp}}(r) \cdot \nabla n_i(r) / n_i(r)$$

where n_e in 10^{13} cm^{-3} . Modeling well describes both relatively flat and sufficiently peaked OH impurities profiles depending on plasma parameters. OH profiles are used as initial conditions for modeling dynamics and steady state in ECRH stage. Experimental data on impurities concentration profiles and particle sources was used for the evaluation of transport parameters. Data on ionization sources of nuclei is obtained from radial profiles of passive linear emission of hydrogen-like ions. Modeling includes recombination sink at the periphery by charge exchange by main gas atoms. For describing both steady states and time dynamics, it was needed to add anomalous diffusion coefficient $D_{\text{an}} \approx 1.5 \text{ m}^2/\text{s}$ with corresponding $V_{\text{an}}(r)$, obtained from ECRH steady state profile. Such anomalous transport almost eliminates neoclassical impurities transport, flattens concentration profiles, and makes them similar to n_e profile in steady state of ECRH after ~ 100 ms after ECRH switch-on. As it can be seen in FIG.12, modeling of radial distribution of carbon and oxygen nuclei in OH and ECRH plasmas is in good agreement with experimental data. Fast removal of initial high central values of concentration in first tens of milliseconds is well described in transport model.

Removal of impurities using ECRH

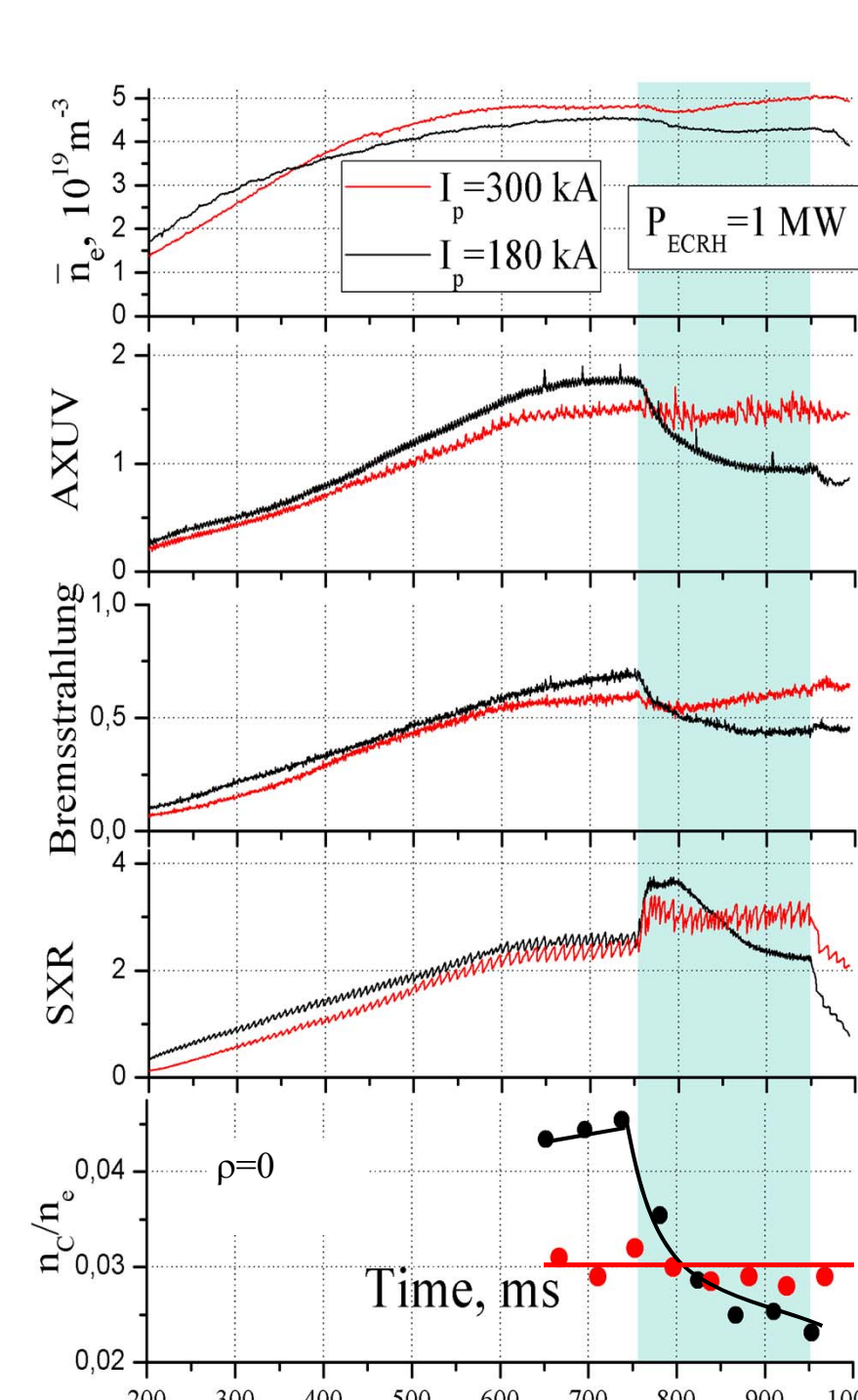


FIG. 7. Evolution of plasma parameters in discharges with $I_p=180$ kA, 300 kA, and $P_{\text{ECRH}}=1$ MW (switched on at 750 ms)

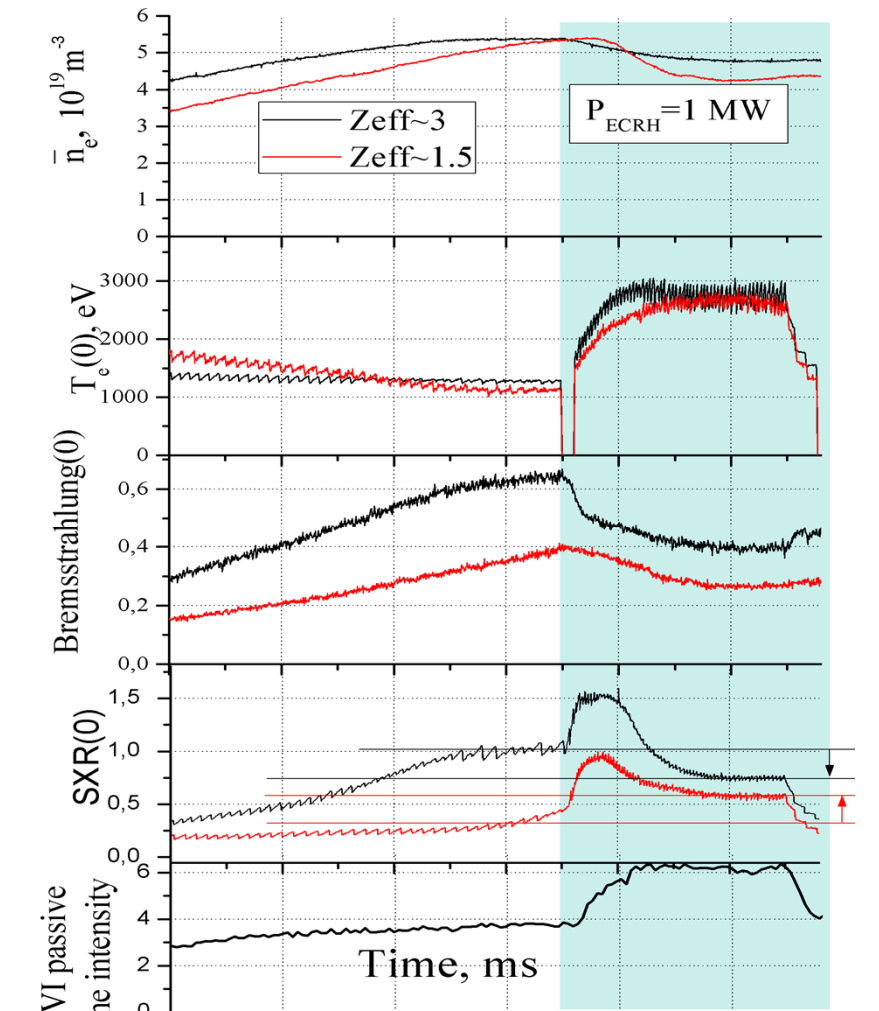


FIG. 8. Evolution of plasma parameters in discharges with $I_p=220$ kA, $P_{\text{ECRH}}=1$ MW (switched on at 750 ms) and two different values of Z_{eff}

Impurity pump-out after switching on the ECR heating is observed in discharges with initial peaking of the impurity nuclei in OH stage. Efficiency of nuclei ejection raises with the increase of \bar{n}_e/I_p ratio, i.e. with the increase of the neoclassical effects that lead to the peaking of impurity nuclei.

Dependence of the impurity pump-out effect on the plasma current

There is a strong tendency in the plasma behavior in discharges with high and low plasma current at the ECRH stage (see FIG.7). Direct CXRS measurements shows decrease of central relative concentration of carbon by a factor of 2 in discharges with low current. Removal of impurities can be clearly seen by bremsstrahlung, SXR and AXUV diagnostics. And there are no significant effects on impurities in the case of high plasma current. In the high plasma current, electron density profile is flat; and in the low current – much more peaked. At the same time, in the case of high current, impurity profiles are similar with electrons profile, and at low current they are significantly sharper than $n_e(r)$. Accordingly, impurity peaking at the high and low plasma currents differs stronger than the peaking of $n_e(r)$ that determines the efficiency of the ECRH impurity pump-out. This fact indicates the predominance of the diffusion component in the impurities removal during ECRH.

Dependence of the impurity pump-out effect on Z_{eff} value

It is necessary to compare the behavior of plasma with high and low values of Z_{eff} . For this, two discharges with plasma current 220 kA and high density ($\bar{n}_e = 5.5 \cdot 10^{19} \text{ m}^{-3}$) were chosen (FIG.8). One of them was provided in usual experimental regime with the high level of Z_{eff} and another one after vacuum vessel lithization (which leads to the reduce of Z_{eff} approximately by a factor of 2). In both discharges, the ECRH power was close to 1 MW. In case of high impurity concentrations, an apparent peaking of the impurity density profile was observed. In the pure plasma, the peaking was not so significant. Density pump-out effect was seen in both discharges, but in the case of the lithization, experiment was provided with switched off gas puff in the ECRH stage, thus decrease of the average density was more substantial. Bremsstrahlung's time evolution shows the abrupt drop of intensity in the first 20 ms that cannot be seen in pure plasma. This effect is connected with the fast removal of impurities from the central region that is not compensated by the increased flux of impurities from the periphery which can be estimated by the emission of the hydrogen-like CVI line. SXR diagnostics shows the decreasing intensity of the emission in the ECRH stage in regard with OH stage despite a significant increase of the electron temperature. In the pure plasma, where impurity density is lower and less peaked, drop of the SXR intensity is significantly lower.

More effective impurity pump-out is observed in higher Z_{eff} and higher impurity gradients discharges.

Dynamics of impurity behavior with ECR heating

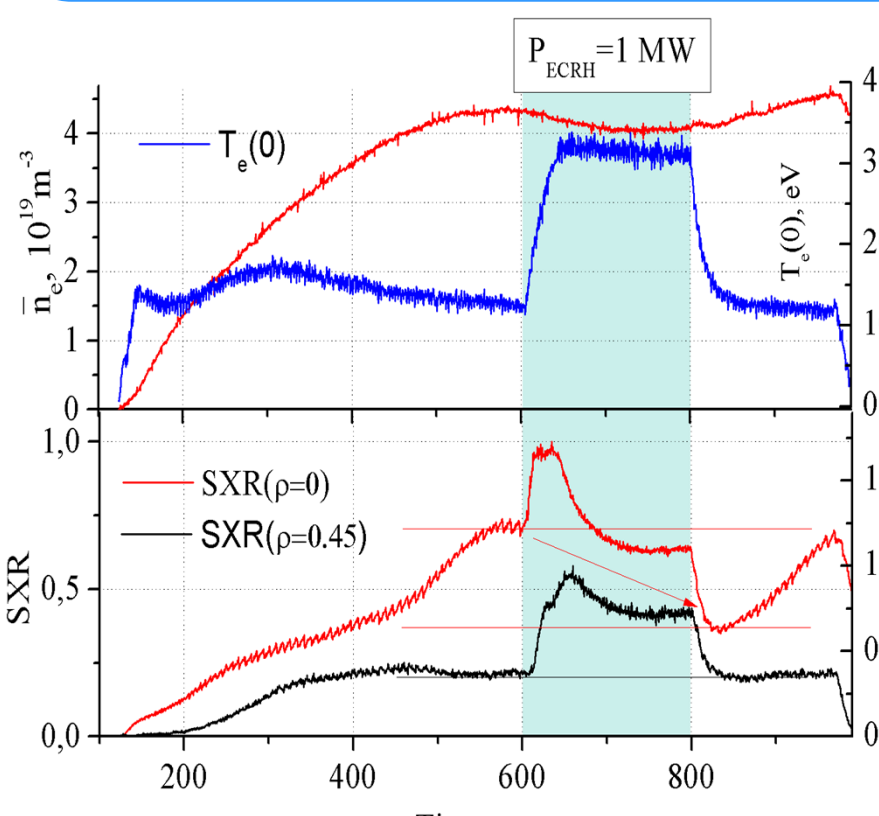


FIG. 9. SXR emission at $\rho=0$ and $\rho=0.45$ in discharge with $I_p=220$ kA, $P_{\text{ECRH}}=1$ MW (switched on at 600 ms)

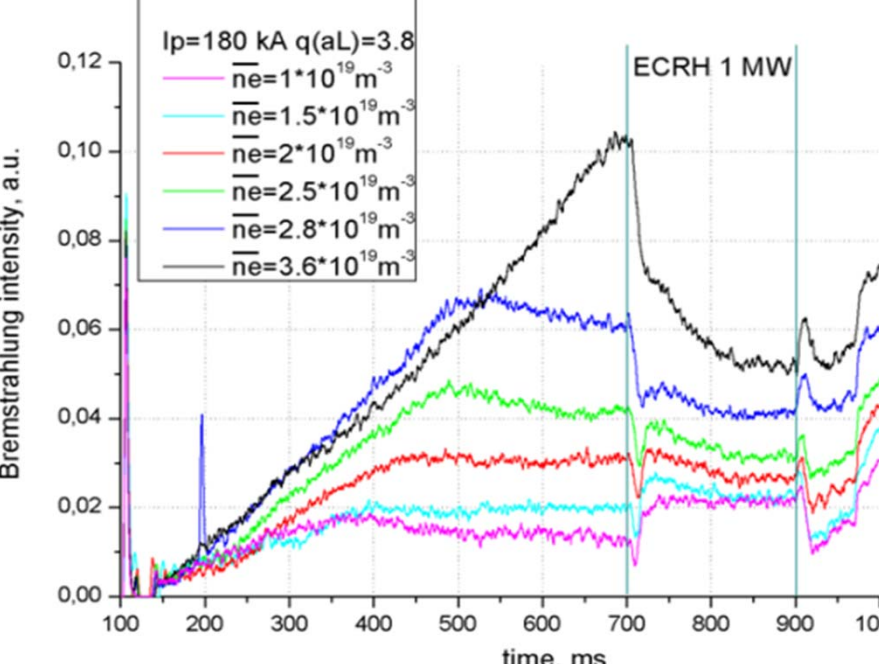


FIG. 10. Bremsstrahlung in discharges with $I_p=180$ kA, $P_{\text{ECRH}}=1$ MW (switched on at 700 ms) and different values of electron density

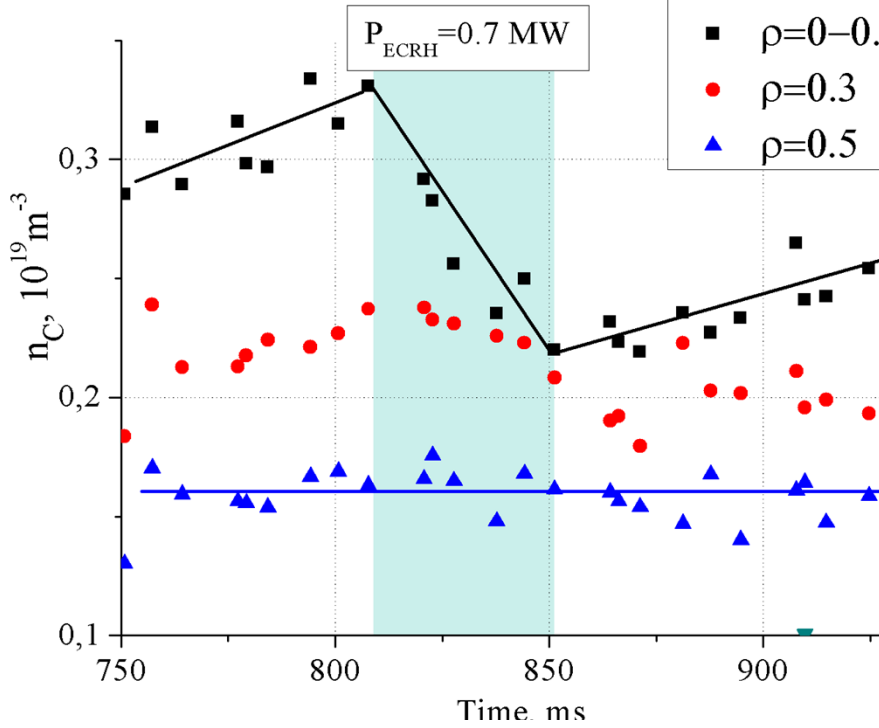


FIG. 11. Carbon concentrations at different radii in discharge with $I_p=180$ kA, $P_{\text{ECRH}}=0.7$ MW (switched on at 810 ms)

Important information about impurity behavior can be obtained from the SXR diagnostics (FIG.9). Relative contribution of light and heavy impurities is difficult to assess, but it can be assumed that heavy impurities (like Fe) are the main contributors to SXR emission. After switching on ECRH, an initial splash of emission is changed by exponential decay with characteristic time $\tau \approx 30$ ms. Dynamics of radial SXR profiles can be used for the estimation of transport parameters of heavy impurities in ECRH. Analysis of this decay is totally identical to the widely used methods of pellet-injection or laser-blow-off injection. The only difference is that excessive concentration of impurities in plasma center is created not by injection into plasma but by neoclassical peaking which is destroyed by ECRH.

Similarly, time interval after switching off ECRH can be used for describing reverse process of peaking in OH plasma. Temperature and density in this interval returns to the initial OH values in time of 50 ms and SXR – in 200 ms, showing the process of peaking.

FIG.10 represents bremsstrahlung dynamics at working ECRH in discharges with plasma current 180 kA where neoclassical peaking is almost always notable at any plasma density. After switching on ECRH, a fast drop of bremsstrahlung is observed.

A set of experiments with ECRH synchronized with diagnostics injector switching-on was performed in order to research these fast processes (see FIG.11).

CXRS measurements show that pump-out of impurities nuclei in the first few tens of milliseconds after switching on central ECRH occurs only in central region of plasma (presumably inside r_s region ≤ 8 cm). It is confirmed by profile measurements of the bremsstrahlung: abrupt initial drop in the intensity at the central chord is observed, and there are no appreciable effects at lines of sight with $\rho \geq 0.25$.

Conclusions

1. Transport of carbon and oxygen nuclei was studied in OH and ECRH discharges at T-10
2. Peaking of impurity nuclei was noticed in experiment that can be related with amplification of the neoclassical impurity transport with regard to anomalous plasma transport
3. Used model with anomalous and neoclassical transport describes experimental profiles of C and O nuclei (and their source and sinks) in wide range changing of n_e , I_p and Z_{eff} parameters at the OH discharge
4. Impurity removal of C and O nuclei was observed at the ECRH discharge and removal efficiency (ratio $n_i^{\text{OH}}(\rho=0)/n_i^{\text{ECRH}}(\rho=0)$) is directly proportional to n_e and Z_{eff} and inversely to I_p
5. Transport model describes removing of C and O nuclei at ECRH discharge with following results:
 - a) In illustrated discharge with ohmic parameters $\bar{n}_e \approx 3 \cdot 10^{19} \text{ m}^{-3}$, $I_p=180$ kA and $Z_{\text{eff}} \approx 4$ it is necessary to use peaked anomalous diffusion coefficient profile (with $D_{\text{an}} \approx 1.5 \text{ m}^2/\text{s}$) for describing dynamics as well as C and O nuclei profile shape
 - b) At ECRH stage initial neoclassical impurity transport is practically disappeared
 - c) Ohmic level of C and O profile peaking affects only to rate of impurity removal at the initial time moment, hence, has little effect on total time to achievement of stationary distribution of impurity nuclei and almost has no effect on the efficiency of removal of C and O nuclei